*Indian J Phys (December 2023) 97(14):4247–4252*
https://doi.org/10.1007/s12648-023-02759-z

ORIGINAL PAPER

# Effect of aluminum nanoparticle size on phase transitions: a molecular dynamics study

**I D Arellano-Ramírez[1,2]*, E A H Ladino[1] and E Restrepo-Parra[2]**

[1]Physics Department, Universidad Tecnológica de Pereira (UTP), Pereira, Colombia

[2]Laboratorio de Física del Plasma, Universidad Nacional de Colombia Sede Manizales, Manizales, Colombia

Received: 12 October 2022 / Accepted: 25 April 2023 / Published online: 29 May 2023

**Abstract:** Isothermal molecular dynamics simulations were carried out with the embedded-atom method as a potential to predict the melting and crystallization temperatures of nanometric sized aluminum particles in the range of 2–4nm. Simulated data predicted a decrease in the melting point $T_m$ of aluminum nanoparticles with an increase in their inverse radius $r^{-1}$ according to an almost linear law. The data obtained predicted a higher value of melting temperature compared to crystallization by $\Delta T = 272$K for a size of 4nm and, $\Delta T = 193K$ for 2nm. The $T_m$ of the nanoparticles augmented with increasing size, from $720K$ for 2nm to 827K for 4nm. Furthermore, a linear extrapolation of the $T_m$ as a function of the inverse of the cubic root of the number of atoms yielded a melting temperature of aluminum of $947 \pm 8$K, which is similar to previous estimations. Finally, when the number of atoms increased the number of face-centered cubic (FCC) structural units also increased, and the amorphous structure decreased.

**Keywords:** Molecular dynamics simulation; Nanoparticles; Melting; Crystallization; Phase transition; Aluminum

## 1. Introduction

Computer simulation has become a fundamental tool in scientific research since it has made possible to describe physical, chemical, and biological phenomena [1, 2]. Specifically, in computational physics, simulations have played a very important role when studying the behavior of nanoparticles since experimental research is difficult to carry out due to their limitations when performing precise experiments at the nanoscale [3]. Therefore, different atomistic simulation techniques such as molecular dynamics (MD) are used. This technique is a powerful tool that can provide physical information to understand phenomena at the atomistic level, that is, it can directly trace the atomic behavior during a phase transition in metals [4–6].

At the nanoscale, the particles exhibit different thermophysical characteristics compared to those found at the microscale. As the size decreases beyond a critical value generated by the increase in the surface-to-volume ratio, the melting point temperature deviates from the value on the macroscopic scale, becoming a size-dependent property [7, 8]. Zhdanov [9] was the first to experimentally observe the hysteresis loop of melting and crystallization for metal samples. Then, Skripov and Koverda [10] carried out a detailed thermodynamic analysis of the problem for small objects in the 1980s. They found an intersection point of the melting curve $T_m$ to be a function of the inverse of the radius of the nanoparticle $r^{-1}$ and the crystallization curve $T_c(r^{-1})$. Since then, several works have shown a reduction in the melting temperature due to the decrease in particle size [11–14]. This is of great importance in determining the ignition and combustion characteristics of nanoparticles [15–20].

In particular, aluminum nanoparticles (AlNp) have different characteristics and applications. They have unusual energetic properties such as higher catalytic activity and higher reactivity [17–19]. In addition, Ivanov and Tepper [21] found that the addition of aluminum nanoparticles can improve the burning rate of propellants by 5 to 10 times more than conventional aluminum particles. The above characteristics contribute to the excess energy of the surface atoms and the reduced activation energy of chemical reactions [22]. All these characteristics are important for the development of next-generation nanoenergetic materials with functional properties [23–27].

*Corresponding author, E-mail: arellano@utp.edu.co

Phase transitions, that is, melting and crystallization hysteresis in nanoparticles are interesting processes because they are different from those in bulk metals. A significant number of studies on the simulation of the particle size effect on AlNp melting have been published [28–34]. Likewise, the effect of AlNp size on solidification has been reported in different studies [3, 35–37]. Although there has been considerable interest in the study of aluminum phase transitions, studies simulating both the melting and crystallization of aluminum nanoparticles are scarce and therefore, the effect of the size of aluminum nanoparticles on a phase transition should be examined. Hence, the purpose of this work was to explore the effect of size on the melting and crystallization temperatures by MD simulation in the canonical ensemble (NVT). In addition, the crystalline structure of AlNp was examined by evaluating the radial distribution function (RDF). Finally, the topological analysis method known as the common neighbor analysis (CNA) was used to track the population of structural units formed during the solidification process.

The article is structured as follows: First, the methodology used to simulate the melting and crystallization process of AlNp for different sizes is explained. Next, the results and discussions about AlNp size under heating and cooling procedures are presented. The final section summarizes the main conclusions.

## 2. Methodology

The MD simulation was carried out using of the free open-source code LAMMPS [38]. The embedded atom model (EAM) was used as an interaction model to describe the aluminum bonds (see Eq. 1) [39]:

$$U = \sum_{i=1}^{N-1} \sum_{j=i+1}^{N} \varphi(r_{ij}) + \sum_{i=1}^{N} \phi(\rho_i) \tag{1}$$

where $\varphi(r_{ij})$ is the pair potential contribution to the cohesive energy as a function of the interatomic distance $r_{ij}$ between atoms $i$ and $j$, and $\phi$ is the energy to embed an atom in a charge density $\rho_i$, where $\rho_i$:

$$\rho_i = \sum_j \psi(r_{ij})$$

where $\psi$ is the contribution from the neighboring atom $j$.

Overall, four MD simulations were carried out in the NVT without periodic boundary conditions, leading to free cluster surfaces [40].

The initial positions of the atoms were assigned randomly, and the initial velocities of each of the atoms were established under a Maxwell–Boltzmann distribution. The equations of motion were integrated using the Verlet algorithm with a time step ($\Delta t$) of $1fs$. Momentum and the angular momentum were removed at each step to avoid involuntary rotation of the aluminum nanoparticles during temperature control. The vibrational temperature control in each step was carried out by implementing a Nose–Hoover thermostat with a temperature damping parameter equal to 100 fs.

**Table 1** Diameter and number of atoms of the simulated AlNp

| Diameter (nm) | $N$ |
|---|---|
| 2.00 | 252 |
| 2.26 | 380 |
| 2.50 | 493 |
| 2.75 | 656 |
| 3.00 | 852 |
| 3.25 | 1082 |
| 3.50 | 1352 |
| 3.75 | 1674 |
| 4.00 | 2048 |

Initially, nanoparticles of 500 randomly distributed atoms were prepared and equilibrated for 4 different relaxation times (0.5, 1.0, 1.5, and 2.0 ns) at a temperature of 300 K. After relaxation, AlNps were heated from 300 to 1000 K at a constant heating rate of 10 K/ps. At a temperature of 1000 K, the system was relaxed for 30 ps and then the crystallization process was started at a cooling rate of 0.2 K/ps until reaching 300 K again.

The best relaxation time was determined to be 1.5 ns based on a smaller variation in crystallization temperatures. Once the relaxation time of 1.5 ns was selected the simulations were performed for different AlNp sizes (see Table 1) and they were calculated according to Eq. (2):

$$rN^{\frac{-1}{3}} = 1.5825 \times 10^{-8} \tag{2}$$

This equation can be obtained using the volumetric density definition $\rho = \frac{m}{V}$, where $m$ is the mass and $V$ is the volume of the nanoparticle. Knowing the atomic weight ($P_A$), Avogadro's number ($N_A$), and the number of atoms (N) we want to simulate, the mass can be calculated, thus:

$$\frac{NP_A}{N_A}\frac{1}{\rho} = \frac{4}{3}\pi r^3$$

And from here, straightforwardly, we can obtain Eq. 2.

For the different sizes of AlNp, the same process of relaxation, heating, relaxation, and subsequent crystallization described above was followed. Afterwards, the crystallized AlNp were subjected to a heating process at a rate of 0.2 K/ps until reaching a temperature of 1000 K again.

The crystallization ($T_C$) and melting ($T_m$) temperatures of the aluminum nanoparticles were determined by analyzing the variations of the potential energy in the crystallization and melting processes. Structural analysis was carried out using the RDF obtained directly from LAMMPS. To carry out a deeper analysis of the AlNp structure for different sizes, the CNA method was used. The free software OVITO [41] was used to visualize the AlNp and the CAN values obtained.

## 3. Results and discussion

The effect of the size of the aluminum nanoparticles on melting and crystallization temperatures is shown in Fig. 1. Both $T_m$ and $T_c$ are linear functions of the reciprocal nanoparticle radius ($r^{-1}$) and, therefore, at $N^{-1/3}$. The deviations of calculated points from a straight line for the $T_m$ dependence are quite small, that is, the nanoparticle size dependence of $T_m$ and $T_c$ agree with the Gibbs–Thomson equation [42, 43] (see Eq. 3). This equation describes the dependence of the melting temperature $T_m$ on the particle radius $r$.

$$\frac{T_m^{\infty} - T_m}{T_m^{\infty}} = \frac{2\sigma_{sl} v_s}{rL^{\infty}} \tag{3}$$

Where $T_m^{\infty}$ is the macroscopic melting temperature, $\sigma_{sl}$ is the solid/liquid interfacial energy, $v_s$ is the specific volume of the solid phase, and $L^{\infty}$ is the macroscopic heat of fusion. Equation 2 is valid for spherical nanoparticles. Skripov [10] made a thermodynamic consideration of phase transition in nanoparticles. According to Skripov, the melting temperature $T_m$ decreases almost linearly with the increment of $r^{-1}$. Figure 1 also shows an intersection point of the curves $T_m$ and $T_c$ for the radius of the nanoparticle that corresponds to a certain characteristic temperature $T_i$. This temperature corresponds to a very small nanoparticle radius $r_i$. A radius of 0.288 nm ($r_i$), which corresponds to $N = 42$ atoms as a point of intersection, was estimated in this study. This value differs from those reported in [10], in which the $r_i$ found was between 0.8 and 1.0 nm.

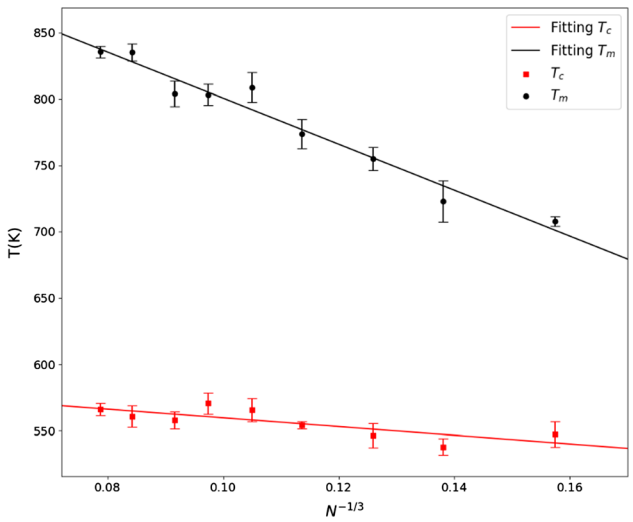


**Fig. 1** Dependence of the melting and crystallization temperatures of aluminum nanoparticles on $N^{-1/3}$

This discrepancy could be due to the different potentials used for the simulations. Furthermore, for an infinite radius of a large particle, that is, for $r^{-1} \to 0$, Fig. 1 does not show a tendency for the melting and crystallization curves to merge at a point that correlates with the melting temperature at bulk, which is equal to the equilibrium temperature $T_0$ between the solid and liquid phases [44]. Linear extrapolation of $T_m(N^{-1/3})$ to $N \to \infty$ yields the macroscopic (bulk) melting temperature. In this study, the bulk melting temperature of aluminum was found to be $947 \pm 8K$, which is comparable to experimental results of 933 K [8].

Figure 2 shows the dependence of the diameter of the nanoparticles in Å and $N^{1/3}$, where N is the number of atoms contained in the nanoparticle. Considering that the melting temperature $T_m$, is proportional to the number of atoms in AlNp as $T_m \propto N^{-1/3}$, the next step was to check whether there is a reasonable relationship between the size of AlNp and the number of atoms. A plot of $d$ as a function of $N^{1/3}$ shown in Fig. 2, yields a linear dependence that satisfies the formula d(Å)=3.199$N^{1/3}$. Hence, obviously, for $N \to 0, d \to 0$.

Figure 3 shows the RDF of the simulated aluminum nanoparticles at 300 K, and under a cooling rate of 0.2 K/ps. According to Fig. 3, when the number of atoms increases from $N = 256$ to $N = 2048$, the position of the first peak dominates and changes slightly from $r = 2.81$ to $r$=2.85Å, respectively. This value is consistent with the

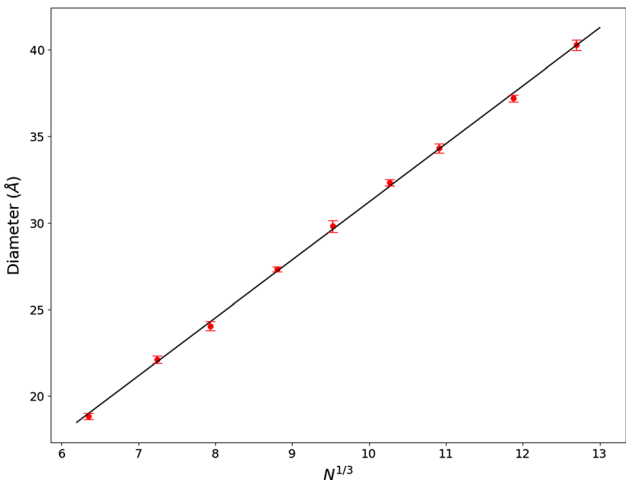


**Fig. 2** Dependence of the aluminum nanoparticle size on $N^{1/3}$

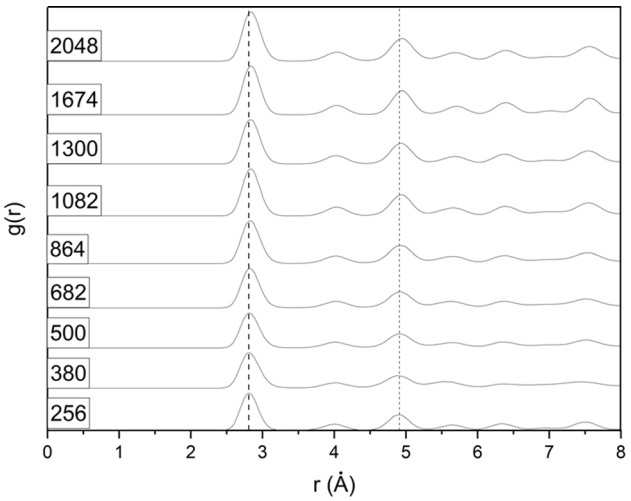


**Fig. 3** Radial distribution function of the simulated nanoparticles at 300 K under a cooling rate of 0.2 K/ps

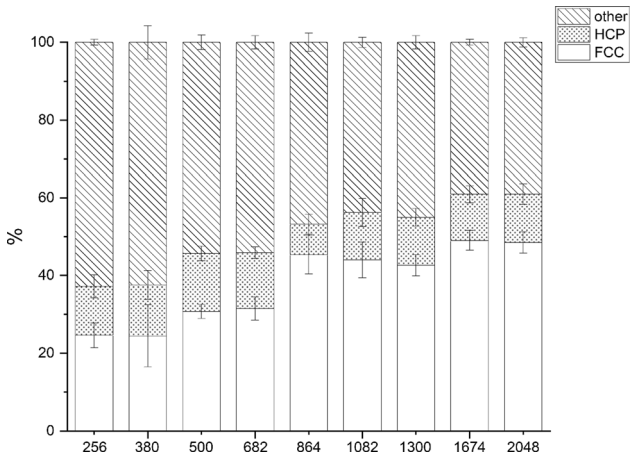


**Fig. 5** Common neighbor analysis method for different sizes of AlNp at 300 K. The values presented are the average of 4 different crystallization simulations. White represents FCC structure; tiny dots represent HCP structure; and oblique lines represent other (amorphous structure)

experimental results of $r = 2.75$ Å [29] and $r = 2.80$ Å [36]. Furthermore, the first peak is narrow (0.62 Å) and regular which indicates that the lattice of aluminum crystal was periodically distributed in the nanoparticles. Also, as the number of atoms increases, $g(r)$ increases slightly. The second highest peak position slightly shifts from $r = 4.91$ to 4.95 Å when the number of atoms increases from $N =$ 256 to 2048.

The shape and the structural units of three simulated AlNp are shown in Fig. 4 (the figures for all the simulated AlNp are presented in the SI). At a cooling and heating rate of $0.2K/ps$ AlNp tends to have an oval shape, in which the atoms are evenly distributed. Figure 4(a) shows an AlNp consisting of $N = 256$ atoms, and a mostly amorphous structure. In Fig. 4(b) ($N = 864$ atoms) the percentage of amorphous structure and FCC structure is equal and, finally, for $N = 2048$ atoms (Fig. 4(c)) about 50% of the structural units are FCC and the amorphous structure is reduced considerably in comparison to the smallest simulated AlNp.

The CNA was used to determine the number of structural units of the AlNp studied. Figure 5 shows that for the smallest nanoparticles, corresponding to Al256 and Al380 atoms, the total percentage of FCC structural units is 24%, around 14% is HCP, and 62% is amorphous (AM). As the number of atoms from Al380 to Al2048 increase, the percentage of the structural units of FCC increases from 24 to 48, the percentage of HCP remains almost unchanged, and the percentage of AM reduces from 62 to 39. The CNA results show that Al1674 and Al2048 have the least number of AM structural units, which indicates that these nanoparticles have the highest crystallization.

The melting-crystallization hysteresis loop was analyzed for the smallest ($N = 256$) and largest ($N = 2048$) simulated AlNp, which are shown in Fig. 6(a) and (b), respectively. $T_c$ significantly differs from $T_m$ in $r^{-1} < r_i^{-1}$, where the melting and crystallization hysteresis curves appear. The essence of this situation is that $T_m$ is greater than $T_c$. The main method to determine $T_m$ and $T_c$ is associated with the detection of jumps in the temperature dependence cohesive energy $U$ of the nanoparticle. In Fig. 6(a) for $N =$ 256 atoms, the melting point was determined from a jump

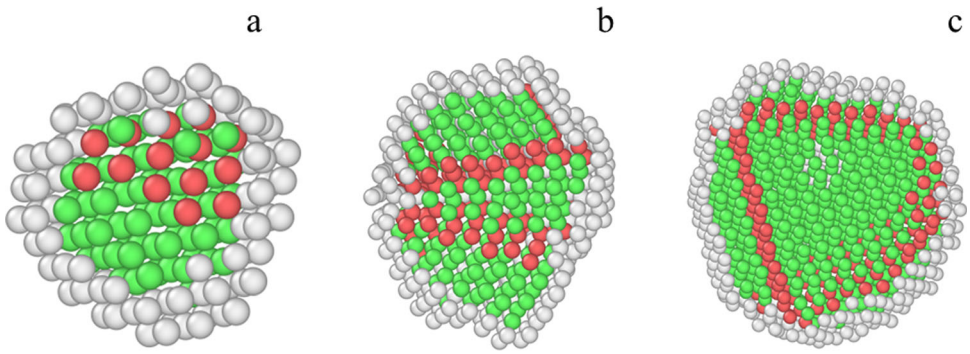


**Fig. 4** Shapes and structural units of the simulated AlNp. (**a**) N = 256 atoms, (**b**) 864 atoms, and (**c**) 2048 atoms. Amorphous structural units are shown in white, FCC structural units in green, and hexagonal close-packed (HCP) structural units in red (color figure online)

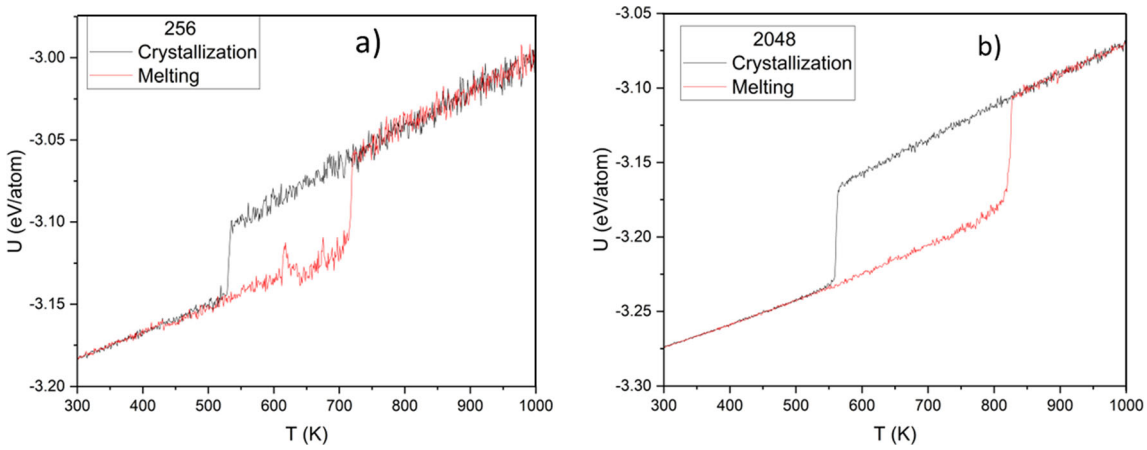


**Fig. 6** Temperature dependence of specific internal energy per atom of (**a**) 256 AlNp atoms and (**b**) 2048 AlNp atoms, demonstrating the melting and crystallization hysteresis loop

in cohesive energy ranging from $-3.11$ to $-3.06\text{eV/atom}$ at a temperature of 720K. Crystallization was determined at a temperature of 527K with a cohesive energy ranging from $-3.10$ to $-3.14\text{eV/atom}$. In this study the temperature difference $\Delta T = T_m - T_c$, which is considered a quantitative measure of the hysteresis, reached $193K$ for AlNp consisting of 256 atoms. In Fig. 6(b), the melting point was determined from a jump in cohesive energy ranging from $-3.18$ to $-3.11\text{eV/atom}$ at a temperature of 827K, which is interpreted as the melting point $T_m$ of AlNp consisting of $N = 2048$ atoms. This AlNp undergoes a crystallization phase transition upon cooling up to 555K, the cohesive energy ranging from $-3.17$ to $-3.23\text{eV/atom}$. The temperature difference $\Delta T = T_m - T_c$ reached 272K for AlNp consisting of 2048 atoms.

Although any hysteresis indicates that the conditions for the corresponding process are not equilibrium, heating and cooling conditions can be treated as quasi-equilibrium conditions for this study, but only in the sense that melting-crystallization hysteresis of pure metals can still be clearly observed for heating and cooling rates of the order of $1\text{K/ps}$ [44] which is in the range of this study.

## 4. Conclusion

Molecular dynamics simulations were conducted to investigate the effect of size on the melting and crystallization temperatures of aluminum nanoparticles. The crystalline structural units of AlNps during the crystallization process were examined using potential energy variation, the radial distribution function, and the common neighbor analysis method.

The Gibbs–Thomson relation appropriately describes the dependence of the melting temperature on the radius of aluminum nanoparticles between 2 and 4 nm in diameter. On the other hand, the macroscopic melting temperature was obtained with an error between 0.6 and 2.3% with respect to the experimental value. This means that the embedded atom method (EAM) proposed by Mendelev [39] adequately models the interatomic interactions, to study phase transitions, of aluminum nanoparticles between 2 and 4 nm of diameter.

In addition, the theoretical predictions made by Skripov and Koverda [10] concerning the behavior of the size dependence of the melting and crystallization temperatures of nanoparticles were observed, namely that at $r^{-1} < r_i^{-1}$, $T_c$ significantly differs from the $T_m$, from where the hysteresis of melting and crystallization curves appears. For the largest simulated AlNp ($N = 2048$) the value of $\Delta T$ was equal to 272K, and for the smallest 193K.

Radial distribution function analysis showed that the $r = 2.85$ Å result is in good agreement with previous results [29, 36]. When the number of atoms increases, AlNp size also increases, the number of FCC structural units increases, and the number of AM structural units decreases, while the HCP structural units remain almost invariable. These results indicate that as the number of atoms increases, the ratio between area and volume decreases yielding the formation of a greater number of FCC structural units.

The authors limited this study to the phase transitions of aluminum nanoparticles that are not located in a particular condensed matter, a consideration that goes beyond the scope of this research.

**Acknowledgements** Authors would like to acknowledge the funding support from Universidad Tecnológica de Pereira (Grant number: 3-22-3) and from Minciencias under the program "Scholarship Bicentennial Doctoral Excellence Program of Colombia-2019".

**Author contributions** IDA-R: Conceptualization, Writing -original draft. EAHL: Data curation, Software. ER-P: Supervision, Funding acquisition.

**Funding** Open Access funding provided by Colombia Consortium.

**Data availability** The authors declare that all data supporting the findings of this study are available within the article and its supplementary information files.

**Declarations**

**Conflict of interest** The authors declare that they have no known competing financial interests or personal relationships that could have appeared to influence the work reported in this paper.



## References

[1] G Wachutka *Sensors Actuators A. Phys.* **41** 279 (1994)
[2] A Borrelli and J Wellmann *NTM Int. J. Hist. Ethics Nat. Sci. Technol. Med.* **27** 407 (2019)
[3] J P Zhang, Y Y Zhang, E P Wang, C M Tang, X L Cheng and Q H Zhang *Chinese Phys. B* **25** 036102 (2016)
[4] M Asta et al *Acta Mater.* **57** 941 (2009)
[5] Y Shibuta, Y Watanabe and T Suzuki *Phys. Lett.* **475** 264 (2009)
[6] Y Watanabe, Y Shibuta and T Suzuki *ISIJ Int.* **50** 1158 (2010)
[7] S Alavi and D Thompson *J. Phys. Chem. A* **110** 1518 (2006)
[8] J Eckert, J C Holzer, C C Ahn, Z Fu and W L Johnson *Nanostructured Mater.* **2** 407 (1993)
[9] G S Zhdanov *Izv. Akad. Nauk* **41** 1004 (1977)
[10] V P Skripov and V P Koverda. *Moscow Izd. Nauk* (1984)
[11] G Cuba-Supanta, J Guerrero-Sanchez, J Rojas-Tapia, C V Landauro, C Rojas-Ayala and N Takeuchi *Mater. Chem. Phys.* **282** 125936 (2022)
[12] N Joshi, N Mathur, T Mane and D Sundaram *Comput. Mater. Sci.* **145** 140 (2018)
[13] Ş Safaltın and S Gürmen *Comput. Mater. Sci.* **183** 109842 (2020)
[14] C Shouqi, Z Haochen, X He and Z Lixin *Mod. Phys. Lett. B* **34** 2150005 (2020)
[15] S Kumar, S K Das and S K Pattanayek *Comput. Mater. Sci.* **152** 393 (2018)
[16] Z Zhang, Y Zheng, H Ye, G Cheng and J Ding *Surf. Interface Anal.* **48** 1423 (2016)
[17] E V Levchenko, A V Evteev, D P Riley, I V Belova and G E Murch *Comput. Mater. Sci.* **47** 712 (2010)
[18] A P Ilin, A A Gromov, V I Vereshchagin, E M Popenko, V A Surgin and H Lehn *Combust Explos. Shock Waves* **37** 664 (2001)
[19] P Song and D Wen *J. Phys. Chem. C* **114** 8688 (2010)
[20] M J Cherukara, K G Vishnu and A Strachan *Phys. Rev. B Condens Matter Mater. Phys.* **86** 075470 (2012)
[21] G V Ivanov and F Tepper *Int. J. Energ. Mater. Chem. Propuls.* **4** 1 (1997)
[22] A Pivkina, P Ulyanova, Y Frolov, S Zavyalov and J Schoonman *Propellants Explos. Pyrotech.* **29** 39 (2004)
[23] S Zhao, T C Germann and A Strachan *J. Chem. Phys.* **125** 164707 (2006)
[24] M A Hobosyan and K S Martirosyan *IEEE Nanotechnol. Mag.* **14** 30 (2020)
[25] H S Kim, J H Kim, K J Kim and S H Kim *Combust. Flame* **194** 801 (2022)
[26] M Li, A Pang, W Li, Y Zhang, X Lv and Z Ma *Combust. Sci. Technol.* **194** 801 (2022)
[27] J Jiang et al *Mater. Chem. Phys.* **273** 125111 (2021)
[28] P Puri and V Yang *J. Phys. Chem. C* **111** 11776 (2007)
[29] L N Kolotova, G E Norman and V V Pisarev *J. Non. Cryst. Solids* **429** 98 (2015)
[30] A V Fedorov and A V Shulgin *Combust. Explos. Shock Waves* **52** 294 (2016)
[31] T T Quoc and D N Trong *Phys. B Condens. Matter* **570** 116 (2019)
[32] J Jiang, P Chen and W Sun *J. Mater. Sci. Technol.* **57** 92 (2020)
[33] Y Liao, M Xiang, X Zhu, J Chen, J Tian and L Ge *Plos One* **15** e0230028 (2020)
[34] A Mahata and M A Zaeem *Model. Simul. Mater. Sci. Eng.* **27** 085015 (2019)
[35] R Sun, P Liu, H Qi, W Wang, F Lv and J Liu *J. Mol. Graph. Model* **100** 107667 (2020)
[36] D Nguyen-Trong and P Nguyen-Tri *J. Mol. Struct.* **1218** 128498 (2020)
[37] S Kiselev *Dokl. Phys.* **61** 47 (2016)
[38] A P Thompson et al *Comput. Phys. Commun.* **271** 108171 (2022)
[39] M I Mendelev, M J Kramer, C A Becker and M Asta *Philos. Mag.* **88** 1723 (2008)
[40] M M Blazhynska, A Kyrychenko and O N Kalugin *Mol. Simul.* **44** 981 (2018)
[41] A Stukowski and K Albe *Model. Simul. Mater. Sci. Eng.* **18** 085001 (2010)
[42] V M Samsonov, S S Kharechkin, S L Gafner, L V Redel' and Y Y Gafner *Crystallogr. Reports* **54** 526 (2009)
[43] G Kaptay *J. Nanosci. Nanotechnol.* **12** 2625 (2012)
[44] V M Samsonov, I V Talyzin and M V Samsonov *Tech. Phys.* **61** 946 (2016)